British Journal of Anaesthesia **113** (S1): i39–i48 (2014)
Advance Access publication 22 May 2014 · doi:10.1093/bja/aeu104

BJA

Potent inhibition by ropivacaine of metastatic colon cancer SW620 cell invasion and $Na_V1.5$ channel function

D. T. Baptista-Hon[1], F. M. Robertson[1], G. B. Robertson[1], S. J. Owen[1], G. W. Rogers[1], E. L. Lydon[1], N. H. Lee[2] and T. G. Hales[1,2]*

[1] The Institute of Academic Anaesthesia, Division of Neuroscience, Medical Research Institute Mailbox 8, Ninewells Hospital, University of Dundee, Dundee DD1 9SY, UK
[2] Department of Pharmacology and Physiology, The George Washington University, 2300 Eye Street NW, Washington, DC 20037, USA
* Corresponding author. E-mail: t.g.hales@dundee.ac.uk

Editor's key points

- Colon cancer cells express voltage gated sodium channels, which mediate invasion.
- This cell culture study evaluated the effect of ropivacaine on voltage gated sodium channels on colon cancer cells.
- Ropivacaine inhibited colon cancer cells' voltage gated sodium channels and invasion, implying a possible role for amide local anaesthetics in cancer surgery.

Background. Metastatic breast and colon cancer cells express neonatal and adult splice variants of $Na_V1.5$ voltage-activated Na^+ channels (VASCs). Block of VASCs inhibits cell invasion. Local anaesthetics used during surgical tumour excision inhibit VASC activity on nociceptive neurones providing regional anaesthesia. Inhibition of VASCs on circulating metastatic cancer cells may also be beneficial during the perioperative period. However, ropivacaine, frequently used to provide analgesia during tumour resection, has not been tested on colon cancer cell VASC function or invasion.

Methods. We used reverse transcription–polymerase chain reaction and sequencing to identify $Na_V1.5$ variants in the SW620 metastatic colon cancer cell line. Recombinant adult and neonatal $Na_V1.5$ variants were expressed in human embryonic kidney cells. Voltage-clamp recordings and invasion assays were used to examine the effects of ropivacaine on recombinant $Na_V1.5$ channels and the metastatic potential of SW620 cells, respectively.

Results. SW620 cells expressed adult and neonatal $Na_V1.5$ variants, which had similar steady-state inactivation profiles, but distinctive activation curves with the neonatal variant having a $V_{1/2}$ of activation 7.8 mV more depolarized than the adult variant. Ropivacaine caused a concentration-dependent block of both $Na_V1.5$ variants, with IC_{50} values of 2.5 and 3.9 μM, respectively. However, the reduction in available steady-state current was selective for neonatal $Na_V1.5$ channels. Ropivacaine inhibited SW620 invasion, with a potency similar to that of inhibition of $Na_V1.5$ channels (3.8 μM).

Conclusions. Ropivacaine is a potent inhibitor of both $Na_V1.5$ channel activity and metastatic colon cancer cell invasion, which may be beneficial during surgical colon cancer excision.

Keywords: colorectal cancer; electrophysiology; ion channels; local anaesthetics

Accepted for publication: 13 February 2014

Colorectal cancer causes ~0.5 million annual deaths worldwide.[1] Death is caused by metastatic spread and up to 75% of fatalities are associated with liver metastases.[2] Surgical tumour excision is the primary treatment for colorectal, breast and prostate cancer. However, surgery can liberate malignant cells into the circulation and disease prognosis is negatively correlated with the number of circulating cancer cells.[3 4] Circulating cancer cells can either generate metastatic tumours in distant tissues or self-seed at the original tumour site, a process that participates in non-metastatic cancer progression.[5] Approaches that reduce the perioperative spread of tumour cells, by inhibiting invasion, may significantly prolong disease-free survival after surgery.

Recent studies suggest that the use of regional anaesthesia (e.g. paravertebral and epidural block) during surgical tumour excision reduces the likelihood of cancer recurrence and metastasis.[6–9] Local anaesthetics administered in this way provide pain relief, an approach that reduces the requirement for general anaesthesia and opioid analgesia. General anaesthesia and opioids may suppress the patient's immune response and inhibit natural killer cells possibly increasing the survival of circulating cancer cells during the perioperative period. These cells may reseed and/or metastasize to additional tissues. The ability of spinal local anaesthetics to reduce the requirement for general anaesthesia and opioids may contribute to their beneficial effects during cancer surgery.[9]

Local anaesthetics relieve pain by inhibiting voltage-activated Na^+ channels (VASCs) on nociceptive neurones; however, local anaesthetics also affect ion channels on other cells. Breast, colon, and prostate cancer cells express local anaesthetic-sensitive VASCs.[10–13] There are several genes that express different VASCs in distinct tissues. We previously

demonstrated that metastatic colon cancer cells express the cardiac $Na_V1.5$ VASC α subunit.[13] Primary colon cancer (SW420) cells have lower levels of $Na_V1.5$ expression than metastatic (SW620) cells isolated from the same patient. Moreover, the level of $Na_V1.5$ expression correlates with their invasive potential. Inhibition of $Na_V1.5$ channels either by applying lidocaine or by siRNA-mediated knockdown reduces SW620 cell migration through a Matrigel membrane, an *in vitro* assay of metastatic invasion.[13]

The local anaesthetic ropivacaine is frequently used to provide regional anaesthesia during surgical tumour excision. However, the effects of ropivacaine have not been tested on $Na_V1.5$ VASCs expressed by metastatic colon cancer cells. In this study, we identified $Na_V1.5$ VASC splice variants in SW620 cells and examined their sensitivities to block by ropivacaine. We also determined that ropivacaine potently inhibits the invasion of SW620 cells.

Methods

Cell culture and transfection

Human embryonic kidney (HEK293) cells and SW620 cells were obtained from American Type Culture Collection (Manassas, VA, USA) and cultured in Dulbecco's Modified Eagle Medium (DMEM) supplemented with 10% fetal bovine serum and 1% penicillin/streptomycin (Invitrogen, Paisley, UK) at 37°C and 5% CO_2. Adult and neonatal $Na_V1.5$ cDNAs were subcloned into pcDNA3.1 vector (Invitrogen). As previously described, HEK293 cells were transfected using calcium phosphate precipitation with cDNA encoding green fluorescence protein to identify transfected cells.[14] For immunocytochemistry, cells were seeded onto poly-L-lysine-coated coverslips in 24-well plates and transfected using lipofectamine (Invitrogen). Mock transfections were performed, as necessary, using empty pcDNA3.1 vector.

Molecular biology

Total RNA from transfected HEK293 cells or SW620 cells was isolated using RNeasy (Qiagen, Manchester, UK) and reverse transcribed (RevertAid RT–PCR Kit, Thermo Scientific, Loughborough, UK) using a single reverse primer for the exon 10–11 boundary (primer P1, Table 1) of human SCN5A (RefSeq NG_008934.1). Single-stranded cDNAs were subsequently amplified by polymerase chain reaction (PCR) with high-fidelity Pfu polymerase (Thermo Scientific, Loughborough, UK) using primer P1, together with forward primers directed against the boundary of exon 5 and either exon 6A (primer P2, Table 1) or exon 6B (primer P3, Table 1) of human SCN5A. PCR products were analysed by agarose gel electrophoresis. Fragments corresponding to exon 6A and 6B were extracted from the gel and sequenced by the Ninewells Hospital Genetics Core Services Unit. To create pcDNA3.1-n$Na_V1.5$, we amplified mRNA fragments containing either exon 6A or 6B from SW620 spanning two unique restriction sites (*Xho*I and *Eco*RI) within the open reading frame of SCN5A using primers P4 and P5 (Table 1). The fragments were replaced into the same region of pCDNA3.1-$Na_V1.5$. The mixed population of plasmids (containing different cDNAs with exons 6A and 6B) were transformed into DH5α (Invitrogen), and screened by colony PCR with primers P1 and P2, which specifically amplifies fragments containing exon 6A (0.53 kb in size). Twenty out of 30 colonies screened contained exon 6A.

Table 1 Primers used for RT–PCR

Primer	Direction	Nucleotide sequence (5′–3′)
P1	Reverse	gga cct gag ggt ctg ctg ata gag
P2	Forward	atc atg gcg tat gta tca gaa aat
P3	Forward	atc atg gcg ta caca act gaa ttt
P4	Forward	tgg acc aag tat gtc gag
P5	Reverse	ctg tga aaa tcc ctg tga

Immunocytochemistry

HEK293 cells or SW620 cells on coverslips were fixed using 2% paraformaldehyde and incubated with a mouse anti-$Na_V1.5$ antibody (ASC-005, Alomone labs, Jerusalem, Israel) at a 1:1000 dilution. An anti-mouse secondary antibody conjugated to Alexa Fluor 488 (Invitrogen) was used to visualize primary antibody binding on a Leica SP-5 confocal microscope at 63× magnification. All image analyses were performed using ImageJ software (http://rsb.info.nih.gov/ij/index.html).

Electrophysiology

The whole-cell patch-clamp technique was used to record voltage-activated Na^+ currents from HEK293 cells expressing recombinant $Na_V1.5$ channels. A non-technical description of the patch-clamp technique is provided in the Supplementary material. The electrode solution contained (in mM) CsCl 130, NaCl 15, $MgCl_2$ 2, EGTA 10, and HEPES 10 (pH 7.4 with CsOH). Glass electrodes were fabricated using borosilicate glass capillaries and when filled with electrode solution had resistances of 1.3–2.3 MΩ. Cells were continually superfused with extracellular solution containing (in mM) NaCl 140, KCl 4.7, $MgCl_2$ 1.2, $CaCl_2$ 2.5, glucose 11, and HEPES 10 (pH 7.4 with NaOH). Currents were recorded using an Axopatch 200B amplifier, low-pass filtered at 2 kHz, digitized at 20 kHz using a Digidata 1320A interface, and acquired using pCLAMP8 software (Molecular Devices, CA, USA). Current–voltage relationships were recorded with depolarizing steps from −80 to 70 in 10 mV increments. Steady-state inactivation data were recorded from cells exposed to 100 ms prepulses to voltages between −140 and −10 mV before the activation voltage of 0 mV. Only currents with a peak amplitude of <5 nA were included for analysis and ≥80% series resistance compensation was used to minimize voltage errors. The perforated patch-clamp technique was used to establish the resting membrane potential of SW620 cells using 300 $\mu g\ ml^{-1}$ amphotericin B, added to the electrode solution which contained (in mM): KCl 145, $MgCl_2$ 1.2, $CaCl_2$ 2.5, glucose 10, and HEPES 10 (pH 7.4 with KOH). Membrane potentials were recorded under current-clamp

conditions and corrected for the calculated liquid junction potential.

Invasion assay

The Matrigel invasion assay was used to investigate SW620 invasion. Boyden invasion chambers (BD Biosciences, Oxford, UK) were coated with Matrigel. SW620 cells were resuspended in DMEM containing 0.1% FBS. DMEM containing 10% FBS was used as a chemoattractant. Chambers were incubated for 48 h at 37°C. Invading cells were fixed in 100% methanol and stained using 1% toluidine blue. Membranes were mounted onto coverslips and imaged using light microscopy. From each membrane, the number of cells in six random fields was counted using an inverted microscope at 10× magnification. Counting was performed under blinded conditions.

Analysis

Current amplitudes were measured using pCLAMP8 software. Activation curves were derived from current–voltage relationships. Na^+ conductances were calculated by determining the driving force at each holding potential (up to 20 mV) established from the Na^+ equilibrium potential. Conductances were normalized to peak values in each cell. Steady-state inactivation data were normalized to peak. Activation and inactivation data were fitted with the Boltzmann functions.[14] Ropivacaine concentration–response data were fitted with a logistic function. Fit parameters were determined from data acquired from individual cells, and expressed as the mean [standard error of the mean (SEM)]. Statistical analyses were performed using the paired or unpaired *t*-test, or one-way analysis of variance (ANOVA), as appropriate. Fitting and statistical analyses were performed using GraphPad Prism software (La Jolla, CA, USA).

Results

SW620 colon cancer cells express adult and neonatal $Na_V1.5$ variants

Our previous immunocytochemical analysis of SW620 cells demonstrates that they express $Na_V1.5$ VASCs.[13] We used a similar approach here to detect $Na_V1.5$ protein in SW620 cells and HEK293 cells transfected with cDNAs encoding either the adult or neonatal $Na_V1.5$ splice variant (Fig. 1A). The antibody labelled SW620 cells and both recombinant $Na_V1.5$ splice variants. We previously detected mRNA encoding the adult $Na_V1.5$ splice variant in SW620 cells.[13] Here, we designed primers specific for the alternatively spliced variants encoded by exons 6A (neonatal) and 6B (adult), respectively (Fig. 1B; Table 1). There was no detectable neonatal $Na_V1.5$ transcript in mock-transfected HEK cells or in those transfected with cDNA encoding the adult $Na_V1.5$ splice variant (Fig. 1C, left and middle panels). These data demonstrate that the primer for the neonatal $Na_V1.5$ splice variant is specific and does not amplify the adult variant. In contrast, we detected transcripts for both the adult and neonatal $Na_V1.5$ splice variants in SW620 cells (Fig. 1C, right panel). Sequencing of the PCR product confirmed that both variants were indeed present. We constructed the full-length cDNA encoding the neonatal $Na_V1.5$ splice variant by replacing nucleotides for exon 6B with those of exon 6A from SW620 transcripts (see the Methods section). Sequencing confirmed successful incorporation of exon 6A and this construct was used for immunocytochemistry in Figure 1A and for comparison with adult $Na_V1.5$ in subsequent electrophysiological experiments.

Functional properties of adult and neonatal $Na_V1.5$ VASCs

Since SW620 cells contain adult and neonatal splice variants of $Na_V1.5$, it is necessary to establish the properties of each VASC subtype. We used the whole-cell patch-clamp technique to characterize Na^+ currents mediated by recombinant adult and neonatal $Na_V1.5$ VASCs expressed either alone or in combination in HEK293 cells. Currents were activated by depolarizing cells from −80 mV to between −70 and +70 mV in 10 mV increments (Fig. 2A). The plot of current density *vs* voltage reveals that the peak amplitude occurred at −10 and 0 mV for adult and neonatal $Na_V1.5$ channels, respectively (Fig. 2B). There was no difference between the peak current density values obtained from cells expressing either variant (Table 2). Activation curves were generated by plotting the conductance at each voltage (normalized to maximum conductance) from HEK293 cells expressing recombinant $Na_V1.5$ channels. The mean values for $V_{1/2}$ of activation (SEM) were established from the Boltzmann fits to data recorded from each cell (Table 2). Figure 2C represents the averaged activation curves for adult and neonatal $Na_V1.5$ channels both alone and in combination. Consistent with previous reports, neonatal $Na_V1.5$ channels exhibited a significantly more depolarized $V_{1/2}$ of activation compared with adult $Na_V1.5$ channels (Fig. 2C and Table 2).[15] Interestingly, in HEK293 cells transfected with equal amounts of cDNAs encoding the adult and neonatal variants, the $V_{1/2}$ of activation of $Na_V1.5$ channels resembled that determined from cells expressing neonatal $Na_V1.5$ channels alone.

Steady-state inactivation data were recorded from HEK293 cells expressing adult and neonatal $Na_V1.5$ splice variants, either alone or in combination (Fig. 2D). Cells were exposed to 100 ms prepulses to voltages between −140 and −10 mV, as illustrated in the inset voltage protocol (Fig. 2A). There was no significant difference between the values for $V_{1/2}$ derived from the Boltzmann fits to the inactivation curves (Table 2). When superimposed, the activation and inactivation curves reveal the window current (Fig. 2E). The region bounded by the curves indicates a range of steady-state voltages at which tonic current is available. Using amphotericin B perforated patch technique under current-clamp conditions, we found the membrane potential of SW620 cells to be −42 (8) mV (n=4). The window current plots indicate a greater available steady-state current at −40 mV for neonatal compared with adult $Na_V1.5$ channels (Fig. 2E). Indeed, as predicted by the window current analysis, the average residual current amplitudes remaining at the end of 20 ms voltage steps to −40 mV were significantly greater in cells expressing neonatal $Na_V1.5$ channels alone or in combination with adult $Na_V1.5$

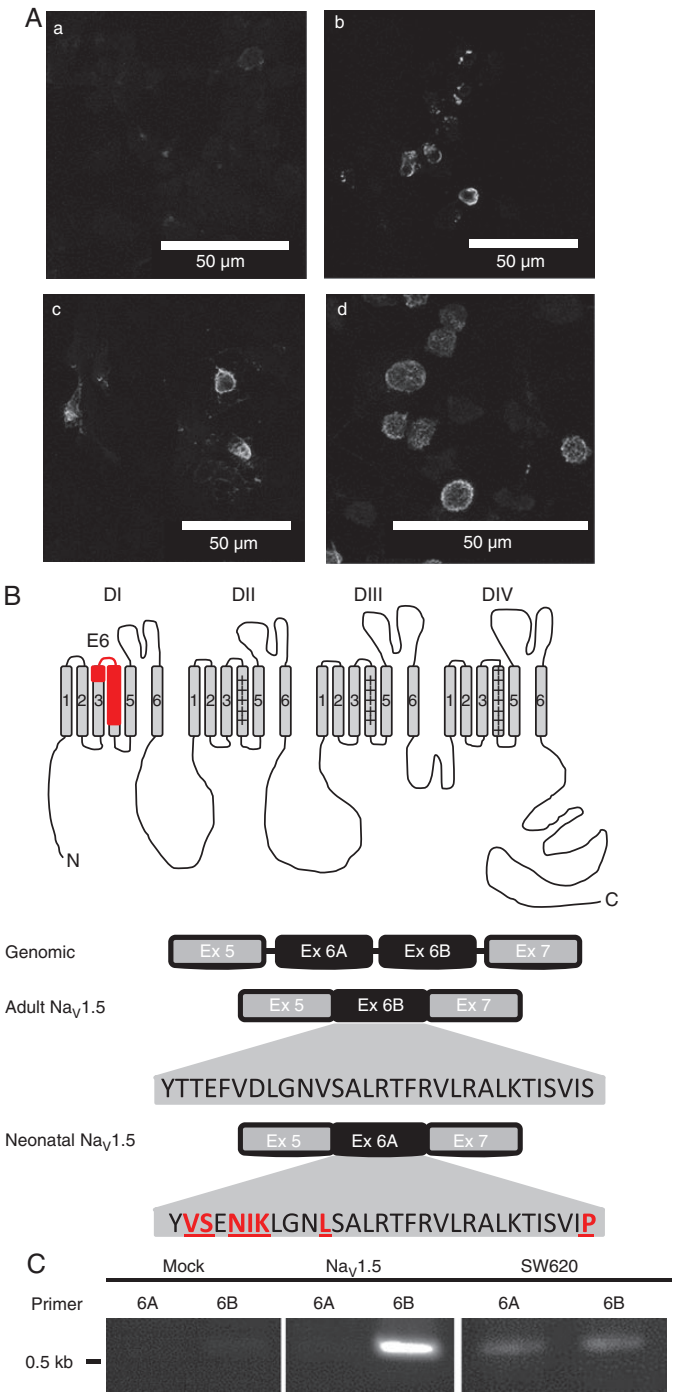

Fig 1 SW620 colon cancer cells express adult and neonatal variants of the $Na_V1.5$ channels. (A) $Na_V1.5$ immunofluorescence in (a) mock, (b) $Na_V1.5$, and (c) $nNa_V1.5$ transfected HEK cells. SW620 colon cancer cells (d) also show strong $Na_V1.5$ immunofluorescence. (B) The top panel illustrates the topology of the $Na_V1.5$ α subunit, with the region affected by alternative splicing of exons 6A and 6B highlighted in red. Exon 6 encodes part of the voltage sensor in the first domain of $Na_V1.5$ channel.[15] The lower panels illustrate the exon structure of adult (middle) and neonatal (bottom) isoforms of $Na_V1.5$. Alternative usage of either exon 6A or exon 6B leads to mRNA encoding $nNa_V1.5$ (neonatal) or $Na_V1.5$ (adult), respectively. The amino acid sequences encoded by the two exons are provided with non-conserved residues highlighted in red. (C) Ethidium bromide-stained DNA from RT–PCR products of mock or $Na_V1.5$-transfected HEK cells and SW620 cells. Either exon 6A or exon 6B specific primers were used. The presence of either exon 6A or exon 6B resulted in a 0.53 kb band. $Na_V1.5$-transfected HEK cells yielded a strong 0.53 kb band only when the exon 6B specific primer was used. SW620 cells yielded 0.53 kb bands when either exon 6A or 6B primers were used, suggesting that SW620 cells contain mRNA transcripts for $Na_V1.5$ and $nNa_V1.5$. Subsequent sequencing of these bands revealed that they indeed correspond to exon 6A and exon 6B of SCN5A, respectively.

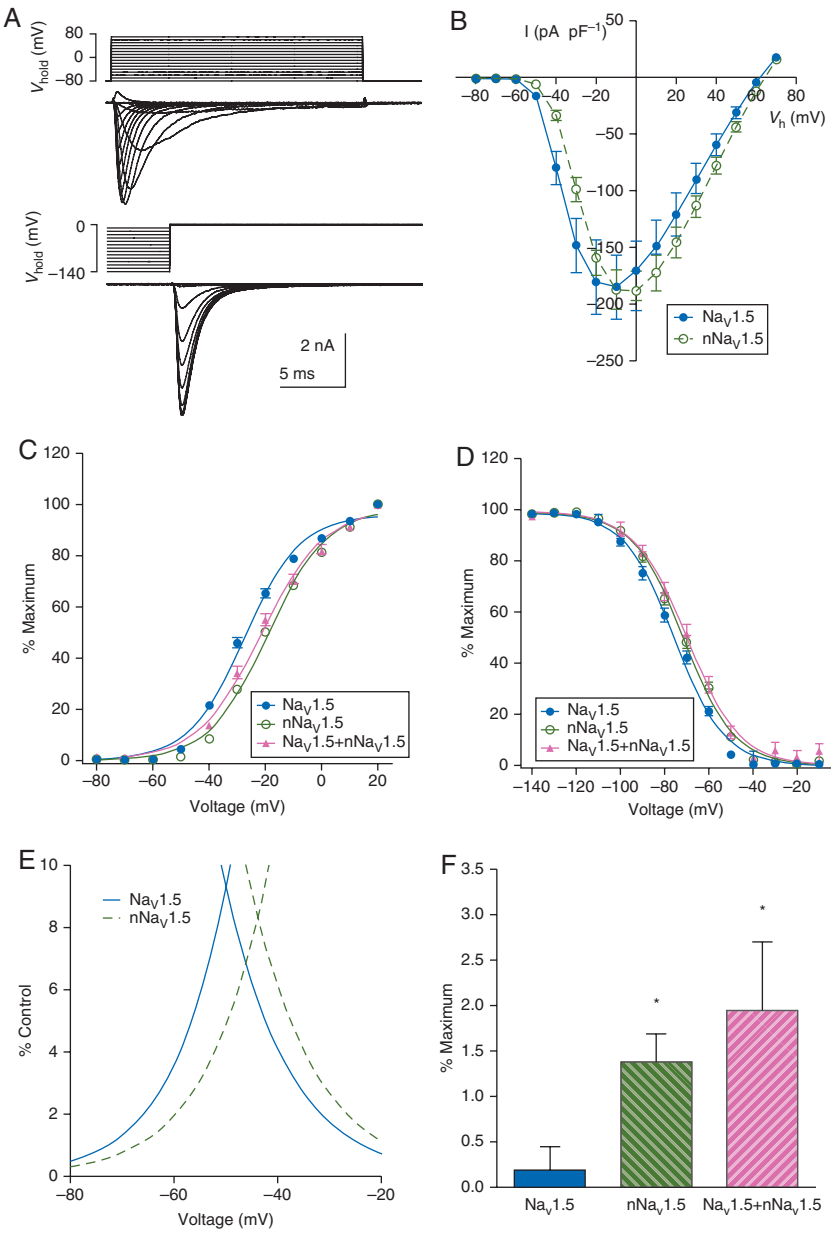

Fig 2 Electrophysiological properties of adult $Na_V1.5$ and neonatal $Na_V1.5$. (A) Representative traces of currents recorded from HEK293 cells expressing recombinant $nNa_V1.5$. The top panel shows the voltage protocols (and corresponding currents) from which the voltage-dependence of activation was established. The bottom panel shows the voltage protocol for recording the voltage-dependence of inactivation. (B) The current–voltage relationship of $Na_V1.5$ (solid circles and line) and $nNa_V1.5$ (open circles and dashed line). The data for $nNa_V1.5$ lie to the right of those for adult $Na_V1.5$, the maximum current occurs at a more depolarized potential. (C) Voltage-dependence of activation. Conductances (derived from the current–voltage relationships) were plotted as a percentage of the respective maximum conductances. A Boltzmann function was fitted to the data. Fitting parameters are summarized in Table 2. Data for $nNa_V1.5$ (open circles) exhibit a significantly dextral-shifted voltage-dependence of activation when compared with $Na_V1.5$ data (solid circles). When $Na_V1.5$ and $nNa_V1.5$ were co-expressed (triangles), the voltage-dependence of activation resembles that of $nNa_V1.5$ expressed alone. (D) Voltage-dependence of inactivation. Currents evoked using the voltage protocol in (A, bottom panel) were converted into conductance values and plotted as a percentage of maximum. Data were fitted with a Boltzmann function (see fitting parameters in Table 2). The voltage-dependence of inactivation of $Na_V1.5$ (solid circles), $nNa_V1.5$ (open circles), and a combination of both isoforms (triangles) did not significantly differ (Table 1). (E) Plots of current availability (window currents) highlighting the region bounded by the Boltzmann fits of activation and inactivation for $Na_V1.5$ (solid lines) and $nNa_V1.5$ (dashed lines). The peak window current occurs with more depolarized potentials in $nNa_V1.5$ compared with $Na_V1.5$. (F) Sustained current amplitude at −40 mV. Bar graph shows the current remaining (as a percentage of maximum) after a step from a holding voltage of −80 to −40 mV. The residual current is significantly larger in cells expressing $nNa_V1.5$ or both $Na_V1.5$ and $nNa_V1.5$ compared with cells expressing $Na_V1.5$ alone ($P<0.05$, one-way ANOVA, *post hoc* Tukey test), consistent with the shift in peak window current seen in (E).

Table 2 Functional characteristics of recombinant $Na_V1.5$ isoforms. $V_{1/2}$ and slope values were taken from the Boltzmann fits to data from individual cells. τ_{inact} was taken from single exponential fits to the maximal current from each cell. Current densities were calculated by dividing the maximum current from each cell by the cell capacitance. Statistical analysis was performed using one-way ANOVA with a *post hoc* Tukey test. The $V_{1/2}$ of activation of $nNa_V1.5$ and the combination of $Na_V1.5$ and $nNa_V1.5$ differed statistically from $Na_V1.5$ alone (*$P<0.05$). All other parameters showed no significant difference.

	$V_{1/2}$ Act (mV)	$V_{1/2}$ Inact (mV)	Activation slope	Inactivation slope	τ_{inact} (ms)	Current density (pA pF^{-1})	*n*
$Na_V1.5$	−27.6 (1.0)	−75.6 (1.3)	9.4 (0.3)	10.1 (0.3)	1.22 (0.06)	213 (28)	39
$nNa_V1.5$	−19.8 (0.7*)	−71.7 (1.1)	10.1 (0.2)	10.6 (0.3)	1.28 (0.08)	191 (17)	42
$Na_V1.5 + nNa_V1.5$	−21.2 (1.5*)	−71.3 (2.5)	10.8 (0.3)	11.7 (1.7)	1.29 (0.10)	156 (46)	10

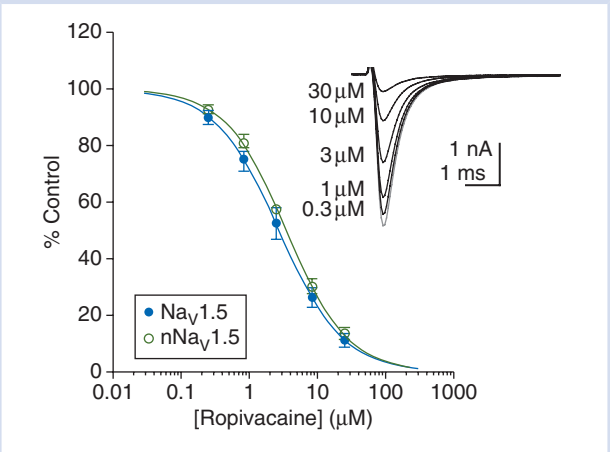

Fig 3 Inhibition of adult $Na_V1.5$ and neonatal $Na_V1.5$ by ropivacaine. The ropivacaine concentration–response relationship for inhibition of $Na_V1.5$ (solid circles) and $nNa_V1.5$ (open circles). The IC_{50} of ropivacaine inhibition was 2.9 (0.7) μM ($n=3$) and 3.5 (0.1) μM ($n=3$). There was no significant difference between the potencies of ropivacaine as an inhibitor of currents mediated by either $Na_V1.5$ or $nNa_V1.5$ ($P>0.1$, *t*-test). Inset shows a representative example of ropivacaine inhibition of $nNa_V1.5$ currents, elicited by a voltage step from −80 mV to 0 mV. The grey trace was recorded in the absence of ropivacaine.

channels, when compared with cells only expressing adult $Na_V1.5$ channels (Fig. 2F).

Inhibition of adult and neonatal $Na_V1.5$ VASCs by ropivacaine

We examined the effects of ropivacaine (0.25–25 μM) on currents mediated by recombinant adult and neonatal $Na_V1.5$ channels expressed in HEK293 cells (Fig. 3). Ropivacaine caused a potent inhibition of both variants. There was no difference in the concentration-dependence of inhibition fitted using a logistics function. The fits yielded IC_{50} values of 2.9 (0.7) μM ($n=3$) and 3.5 (0.1) μM ($n=3$) for adult and neonatal $Na_V1.5$ splice variants, respectively. We investigated whether ropivacaine (2.5 μM) differentially influenced the voltage-dependence of activation or inactivation of the adult and neonatal $Na_V1.5$ variants. Paired recordings before and during steady-state inhibition revealed that ropivacaine suppressed the amplitude of currents mediated by either $Na_V1.5$ variant at all voltages (Fig. 4). Ropivacaine also caused significant shifts in the $V_{1/2}$ of inactivation to more hyperpolarized potentials, which were −80 (5) mV ($n=6$) and −79 (2) mV ($n=5$) for adult and neonatal $Na_V1.5$ channels, respectively (Fig. 4). Ropivacaine had no effect on the $V_{1/2}$ of activation for either variant (Fig. 4). Ropivacaine also reduced the steady-state window current in cells expressing neonatal $Na_V1.5$ channels (Fig. 4). The area under the curve bounded by the activation and inactivation curves was significantly reduced from 159 (24) to 107 (11) ($n=5$, $P<0.05$, paired *t*-test) in cells expressing neonatal $Na_V1.5$ channels. In contrast, the area under the curve bounded by activation and inactivation curves was not significantly influenced by ropivacaine in cells expressing adult $Na_V1.5$ channels ($n=6$, $P>0.1$, paired *t*-test).

Ropivacaine inhibits invasion of SW620 cells through Matrigel

SW620 cells invade through Matrigel, a proprietary matrix used to mimic the epithelial basement membrane.[13] We examined the ability of SW620 cells to invade by using a range of Matrigel concentrations (10–100 μg ml^{-1}). We found that SW620 cells exhibit optimal invasion through a 50 μg ml^{-1} Matrigel membrane (Fig. 5A). We previously demonstrated that tetrodotoxin and lidocaine both inhibit invasion of SW620 metastatic colon cancer cells through Matrigel, suggesting that invasion is attenuated by VASC inhibition.[13] Indeed, this action is likely to be mediated by inhibiting $Na_V1.5$ channels, since selective knockdown of the ion channel's expression using siRNA caused a similar reduction in invasion. We confirmed that lidocaine (10 μM) inhibits invasion at all Matrigel concentrations tested (Fig. 5A). We also examined the effects of the VASC activator veratridine. Veratridine (10 μM) caused a significant increase in SW620 invasion, consistent with a positive contribution of $Na_V1.5$ activity to this process (Fig. 5B). Ropivacaine caused a concentration-dependent inhibition of SW620 invasion. The IC_{50} for the inhibition of SW620 invasion by ropivacaine (determined by fitting the data using a logistics function) was 3.8 μM (Fig. 5C), similar to the IC_{50} for its inhibition of Na^+ currents mediated by $Na_V1.5$ channels (Fig. 3).

Discussion

We demonstrated that SW620 colon cancer cells express adult and neonatal $Na_V1.5$ splice variants. The two variants exhibited

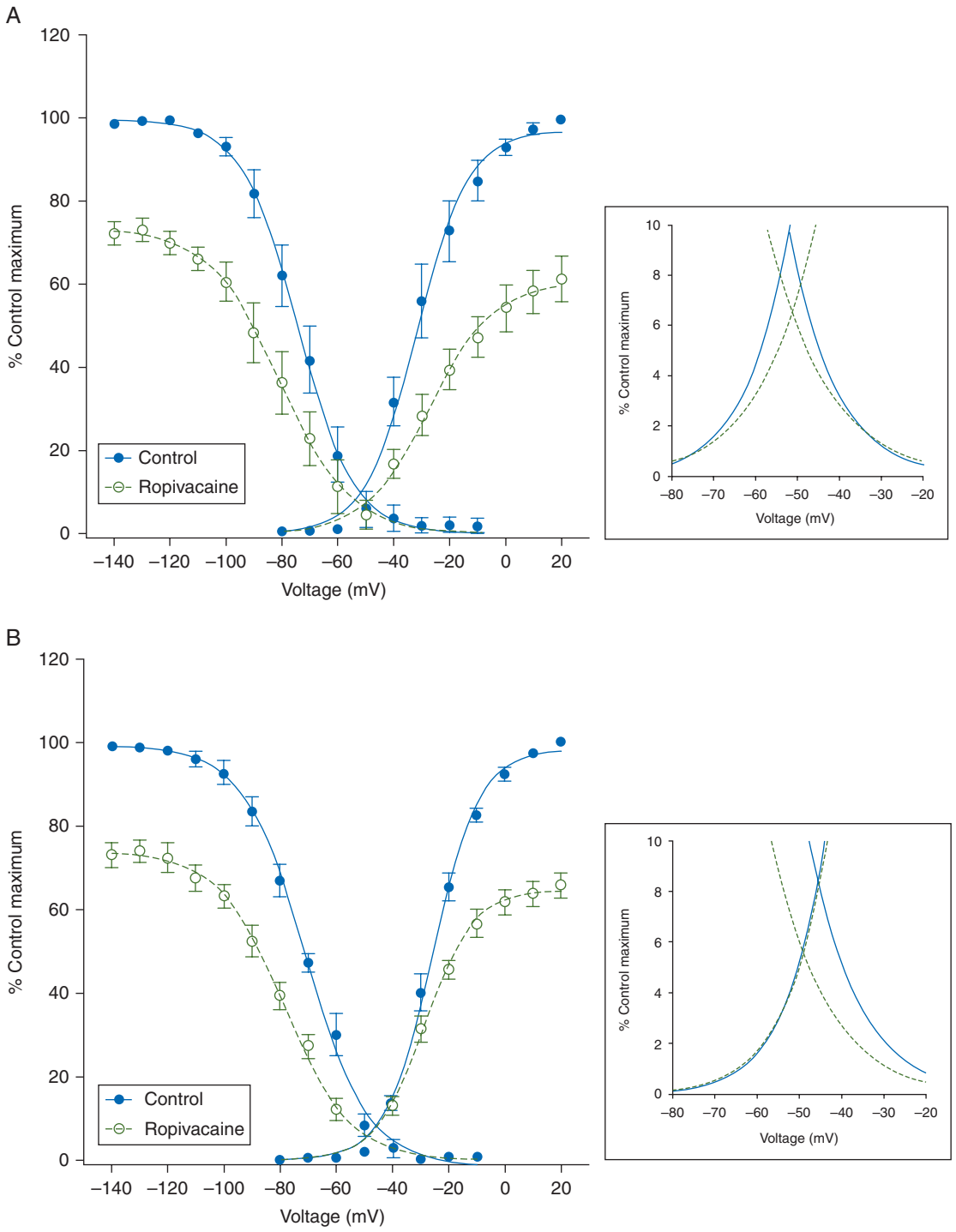

Fig 4 Ropivacaine affects the voltage-dependence of current availability. Voltage-dependence of activation and inactivation and Boltzmann fits were performed as described in Figure 2. Solid circles and lines show the voltage-dependence of activation and inactivation of $Na_V1.5$ (A) and $nNa_V1.5$ (B). Open circles and dashed lines show the voltage dependence of activation and inactivation in the presence of ropivacaine (2.5 μM). Data points were normalized to the maximum under control conditions. Ropivacaine significantly shifted the voltage-dependence of inactivation of $Na_V1.5$ and $nNa_V1.5$ from −74.3 (3.4) mV to −80.3 (4.6) mV ($n=6$; $P<0.05$; paired t-test) and −71.4 (1.8) mV to −78.6 (2.1) mV ($n=5$; $P<0.05$; paired t-test), respectively. There was no statistically significant effect on the voltage-dependence of activation. Inset shows the effect of ropivacaine on the window current. Ropivacaine shifted the peak of the $nNa_V1.5$ window current to more hyperpolarized potentials (see text).

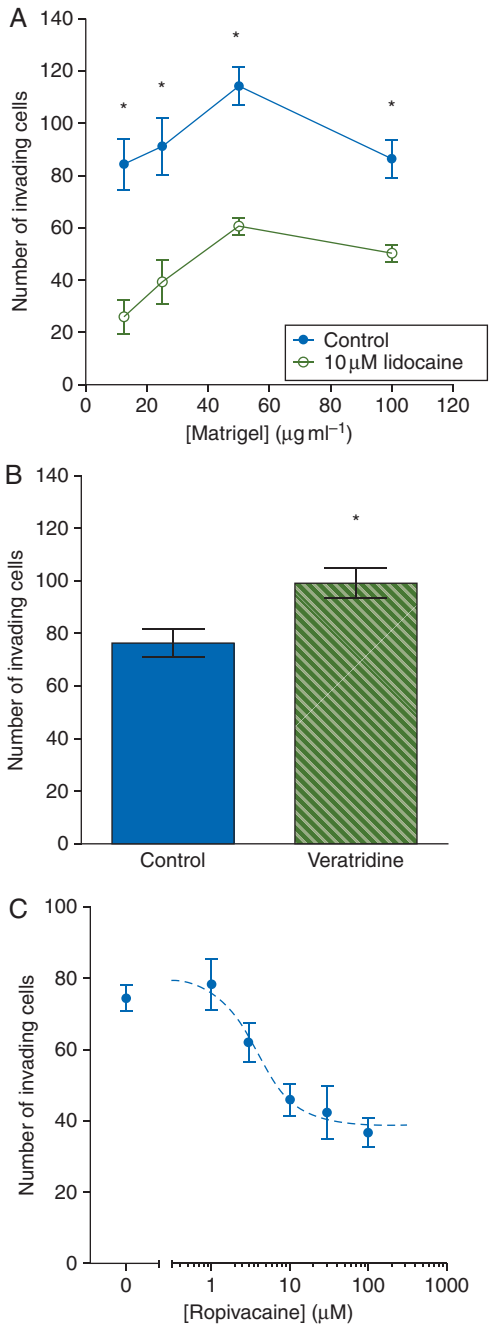

Fig 5 Lidocaine and ropivacaine inhibit SW620 colon cancer cell invasion. (A) SW620 invasion was quantified using a range of Matrigel concentrations. Invasion was optimal with 50 μg ml^{-1} Matrigel. Lidocaine (10 μM) inhibited SW620 cell invasion at all Matrigel concentrations (*$P<0.05$; one-way ANOVA; *post hoc* Tukey test). (B) SW620 invasion is VASC activity dependent. The bar graph shows that the VASC activator veratridine (10 μM) potentiated SW620 invasion ($P<0.05$, *t*-test). (C) Ropivacaine inhibited SW620 invasion. The graph shows the effect of increasing concentrations of ropivacaine on SW620 invasion. The dotted line shows the logistic fit of the concentration–response relationship. The IC_{50} of ropivacaine inhibition of SW620 invasion was 3.8 μM. Invasion was significantly reduced at 10, 30, and 100 μM ropivacaine ($P<0.05$; one-way ANOVA; *post hoc* Dunnett's test *vs* control values).

similar steady-state inactivation profiles, but different values for $V_{1/2}$ of activation. As reported previously, the neonatal variant requires significantly higher voltages for activation.[15] This is consistent with alternative splicing of exon 6 affecting the sequence of the initial voltage sensor. Neonatal $Na_V1.5$ VASCs also mediate a greater proportion of available sustained current at more depolarized potentials, such as −40 mV, the approximate membrane potential of SW620 cells. When expressed together, the functional characteristics of the neonatal variant were dominant. These findings suggest that the neonatal $Na_V1.5$ variant likely mediates a low level of tonic inward Na^+ current in SW620 cells.

Ropivacaine inhibited currents mediated by either adult or neonatal $Na_V1.5$ channels with similar potency. When applied at a concentration close to IC_{50}, ropivacaine inhibited Na^+ currents mediated by either variant, regardless of the holding voltage, shifting inactivation to more hyperpolarized potentials without affecting the voltage-dependence of activation. These findings suggest that ropivacaine inhibits $Na_V1.5$ channels by stabilizing the inactivated state, a common mechanism of high potency block of VASCs by local anaesthetics.[16] Importantly in the context of colon cancer cells, ropivacaine caused a reduction in the availability of sustained current mediated by neonatal $Na_V1.5$ channels. It is this reduction in steady-state current that likely underlies the observed inhibition of SW620 cell invasion through Matrigel. The potency of ropivacaine as an inhibitor of $Na_V1.5$-mediated current and SW620 cell invasion is similar, in keeping with the demonstration that invasive behaviour in SW620 cells requires functional $Na_V1.5$ channels.[13] Consistent with this, the VASC activator veratridine enhanced SW620 invasion through Matrigel.

Retrospective analyses suggest that local anaesthetics reduce the likelihood of cancer recurrence after surgical tumour excision.[6–9] If so, there are several mechanisms that may contribute to their beneficial effect. Regional nerve block reduces the requirement for general anaesthesia and opioids, which may have negative effects on the immune system, the stress response, and/or natural killer cells. Local anaesthetics may also have direct beneficial effects. Some local anaesthetics may be anti-inflammatory and/or interact with second messenger systems to reduce cell proliferation and migration.[17] The presence of VASCs on metastatic cancer cells (including those derived from breast, colon, prostate, and lung tissue) provides another direct target for the beneficial effects of local anaesthetics.[10–13] Our demonstration that ropivacaine potently inhibits the activity of neonatal $Na_V1.5$ channels, a variant expressed by metastatic cancer cells derived from both colon and breast suggests that systemic local anaesthetic might contribute to the apparent beneficial effect of regional anaesthesia during tumour excision.[15] VASCs expressed by cancer cells are likely to be predominantly in the inactivated state, which has a high affinity for local anaesthetics. In contrast, high concentrations of local anaesthetics are required to block impulses in nerves in which VASCs rarely visit the inactivated state.[16] Clinical studies demonstrate that maximum circulating free ropivacaine concentrations after peripheral nerve block and epidural infusion range between 0.2 and 0.7 mg ml^{-1}.[18–22] This equates to a

maximum concentration of 2.4 μM, close to the IC_{50} values for inhibition of both $Na_V1.5$ channel function and SW620 invasion. Therefore, it is possible that during regional anaesthesia, circulating ropivacaine may inhibit $Na_V1.5$ channel function on circulating colon cancer cells, an action that attenuates invasion.

While regional anaesthesia may help reduce cancer recurrence and metastases after tumour excision, direct local anaesthetic administration onto tumours and/or i.v. would likely maximize any direct beneficial effects. A drawback is the possibility of toxicity which occurs largely through the block of ion channels in cardiac tissue. It is ironic that the $Na_V1.5$ channel, which may contribute to beneficial effects of local anaesthetics on metastatic breast and colon cancer cells, is also found in the heart where its block would be detrimental. The presence of the neonatal variant and a predominance of the inactivated state may provide an opportunity to selectively target $Na_V1.5$ channels in cancer cells by the systemic administration of low concentrations of local anaesthetics or other state-dependent VASC inhibitors.

Supplementary material

Supplementary material is available at *British Journal of Anaesthesia* online.

Authors' contributions

D.T.B-H.: performed experiments, data analysis, wrote first draft of manuscript, and study design; F.M.R.: performed experiments and data analysis; G.B.R.: performed experiments and data analysis; S.J.O.: performed experiments and data analysis; G.W.R.: performed experiments and data analysis; E.L.L.: performed experiments and data analysis; N.H.L.: study design and editing manuscript; T.G.H.: study design and wrote final draft of manuscript.

Acknowledgements

We thank Lisa Wright for expert technical assistance and Taha Elajnef for help with immunocytochemistry.

Declaration of interest

None declared.

Funding

This work was supported by a *BJA*/RCoA grant awarded via NIAA to T.G.H.

References

1 Din FV, Theodoratou E, Farrington SM, *et al.* Effect of aspirin and NSAIDs on risk and survival from colorectal cancer. *Gut* 2010; **59**: 1670–9

2 Faerden AE, Sjo OH, Bukholm IR, *et al.* Lymph node micrometastases and isolated tumor cells influence survival in stage I and II colon cancer. *Dis Colon Rectum* 2011; **54**: 200–6

3 Eschwège P, Dumas F, Blanchet P, *et al.* Haematogenous dissemination of prostatic epithelial cells during radical prostatectomy. *Lancet* 1995; **346**: 1528–30

4 Peach G, Kim C, Zacharakis E, Purkayastha S, Ziprin P. Prognostic significance of circulating tumour cells following surgical resection of colorectal cancers: a systematic review. *Br J Cancer* 2010; **102**: 1327–34

5 Kim MY, Oskarsson T, Acharyya S, *et al.* Tumor self-seeding by circulating cancer cells. *Cell* 2009; **139**: 1315–26

6 Exadaktylos AK, Buggy DJ, Moriarty DC, Mascha E, Sessler DI. Can anesthetic technique for primary breast cancer surgery affect recurrence or metastasis? *Anesthesiology* 2006; **105**: 660–4

7 Biki B, Mascha E, Moriarty DC, Fitzpatrick JM, Sessler DI, Buggy DJ. Anesthetic technique for radical prostatectomy surgery affects cancer recurrence: a retrospective analysis. *Anesthesiology* 2008; **109**: 180–7

8 Snyder GL, Greenberg S. Effect of anaesthetic technique and other perioperative factors on cancer recurrence. *Br J Anaesth* 2010; **105**: 106–15

9 Sessler DI, Ben-Eliyahu S, Mascha EJ, Parat MO, Buggy DJ. Can regional analgesia reduce the risk of recurrence after breast cancer? Methodology of a multicenter randomized trial. *Contemp Clin Trials* 2008; **29**: 517–26

10 Laniado ME, Lalani EN, Fraser SP, *et al.* Expression and functional analysis of voltage-activated Na+ channels in human prostate cancer cell lines and their contribution to invasion in vitro. *Am J Pathol* 1997; **150**: 1213–21

11 Fraser SP, Diss JK, Chioni AM, *et al.* Voltage-gated sodium channel expression and potentiation of human breast cancer metastasis. *Clin Cancer Res* 2005; **11**: 5381–9

12 Brisson L, Gillet L, Calaghan S, *et al.* $Na_V1.5$ enhances breast cancer cell invasiveness by increasing NHE1-dependent H^+ efflux in caveolae. *Oncogene* 2011; **30**: 2070–6

13 House CD, Vaske CJ, Schwartz AM, *et al.* Voltage-gated Na+ channel SCN5A is a key regulator of a gene transcriptional network that controls colon cancer invasion. *Cancer Res* 2010; **70**: 6957–67

14 Safa P, Boulter J, Hales TG. Functional properties of $Ca_V1.3$ (α_{1D}) L-type Ca^{2+} channel splice variants expressed by rat brain and neuroendocrine GH_3 cells. *J Biol Chem* 2001; **276**: 38727–37

15 Onkal R, Mattis JH, Fraser SP, *et al.* Alternative splicing of Nav1.5: an electrophysiological comparison of 'neonatal' and 'adult' isoforms and critical involvement of a lysine residue. *J Cell Physiol* 2008; **216**: 716–26

16 Wang GK, Strichartz GR. State-dependent inhibition of sodium channels by local anesthetics: a 40-year evolution. *Biochem (Mosc) Suppl Ser A Membr Cell Biol* 2012; **6**: 120–7

17 Piegeler T, Votta-Velis EG, Liu G, *et al.* Antimetastatic potential of amide-linked local anesthetics: inhibition of lung adenocarcinoma cell migration and inflammatory Src signaling independent of sodium channel blockade. *Anesthesiology* 2012; **117**: 548–59

18 Bleckner L, Solla C, Fileta BB, Howard R, Morales CE, Buckenmaier CC. Serum free ropivacaine concentrations among patients receiving continuous peripheral nerve block catheters: is it safe for long-term infusions? *Anesth Analg* 2014; **118**: 225–9

19 Bleckner LL, Bina S, Kwon KH, McKnight G, Dragovich A, Buckenmaier CC III. Serum ropivacaine concentrations and systemic local anesthetic toxicity in trauma patients receiving long-term continuous peripheral nerve block catheters. *Anesth Analg* 2010; **110**: 630–4

20 Schoenmakers KP, Vree TB, Jack NT, van den Bemt B, van Limbeek J, Stienstra R. Pharmacokinetics of 450 mg ropivacaine with and without epinephrine for combined femoral and sciatic nerve block in lower extremity surgery. A pilot study. *Br J Clin Pharmacol* 2013; **75**: 1321–7

21 Wiedemann D, Mühlnickel B, Staroske E, Neumann W, Röse W. Ropivacaine plasma concentrations during 120-hour epidural infusion. *Br J Anaesth* 2000; **85**: 830–5

22 McCrae AF, Westerling P, McClure JH. Pharmacokinetic and clinical study of ropivacaine and bupivacaine in women receiving extradural analgesia in labour. *Br J Anaesth* 1997; **79**: 558–62

Handling editor: D. J. Buggy